Identification of a micropeptide and multiple secondary cell genes that modulate *Drosophila* male reproductive success

Clément Immarigeon[a,1,2], Yohan Frei[a], Sofie Y. N. Delbare[b], Dragan Gligorov[a], Pedro Machado Almeida[a], Jasmine Grey[b], Léa Fabbro[a], Emi Nagoshi[a], Jean-Christophe Billeter[c], Mariana F. Wolfner[b], François Karch[a], and Robert K. Maeda[a,2]

[a]Department of Genetics and Evolution, Sciences III, University of Geneva, 1211 Geneva 4, Switzerland; [b]Department of Molecular Biology and Genetics, Cornell University, Ithaca, NY 14853-2703; and [c]Groningen Institute for Evolutionary Life Sciences, University of Groningen, Groningen 9700 CC, The Netherlands

Edited by Claude Desplan, New York University, New York, NY, and approved February 3, 2021 (received for review February 6, 2020)

Even in well-characterized genomes, many transcripts are considered noncoding RNAs (ncRNAs) simply due to the absence of large open reading frames (ORFs). However, it is now becoming clear that many small ORFs (smORFs) produce peptides with important biological functions. In the process of characterizing the ribosome-bound transcriptome of an important cell type of the seminal fluid-producing accessory gland of *Drosophila melanogaster*, we detected an RNA, previously thought to be noncoding, called *male-specific abdominal* (*msa*). Notably, *msa* is nested in the HOX gene cluster of the Bithorax complex and is known to contain a micro-RNA within one of its introns. We find that this RNA encodes a "micropeptide" (9 or 20 amino acids, MSAmiP) that is expressed exclusively in the secondary cells of the male accessory gland, where it seems to accumulate in nuclei. Importantly, loss of function of this micropeptide causes defects in sperm competition. In addition to bringing insights into the biology of a rare cell type, this work underlines the importance of small peptides, a class of molecules that is now emerging as important actors in complex biological processes.

smORF peptide | reproduction | accessory gland | postmating response | *Drosophila*

The genomes of higher eukaryotes appear to contain a paradox: most of their nonrepetitive DNA is transcribed, but only a small fraction codes for proteins. While some long noncoding RNAs (lncRNAs) are undoubtedly functional units, it remains controversial whether most lncRNAs have a function or simply reflect transcriptional noise (1). Further complicating this issue, some lncRNAs actually encode small peptides from small open reading frames (smORFs) that were overlooked in early scans for coding genes (2–10). A growing number of cases have been reported where a smORF-encoded peptide is indeed functional (8, 11, 12). In *Drosophila*, several such peptides are critical for the control of development and physiology (13–18). However, the function of most smORF-encoded peptides is still unknown. Overall, the limits of the coding/noncoding and functional/nonfunctional parts of genomes are still blurry, even in the case of model organisms with well-annotated and studied genomes like *Drosophila melanogaster*.

In this study, we report the identification of a functional micropeptide encoded by a putative "noncoding" RNA, from the secondary cells of the *Drosophila* male accessory glands (AGs). AGs produce most of the seminal fluid proteins that are transferred to females during copulation and are critical for reproductive success. AGs are often referred to as functional analogs of the mammalian prostate gland and seminal vesicles (19, 20). In insects, secretions from AGs induce and maintain the physiological and behavioral changes occurring after mating in females, collectively called the postmating responses (PMRs). The PMR includes increased ovulation and egg laying, sperm storage and release, dietary changes, and gut growth. PMR also include decreased receptivity to remating, ensuring propagation of the first male's genome at the expense of rivals (reviewed in refs. 21, 22). Due to their central role in insect reproduction and evolution, AGs and the individual seminal fluid proteins that they produce to mediate the PMR are topics of intense interest. Insights obtained from the *Drosophila* model have proven relevant for other problematic species (21, 23–25), and thus, identification of novel AG products offer important avenues for the benefit of human health and agriculture.

Here, we examined the overall transcriptome and ribosome-associated transcriptome of an important yet cryptic cell type in the AG: the secondary cells (SCs). SCs are large binucleate cells whose cytoplasm is filled with vacuole-like structures (26–29) These cells express specific genes (29) and proteins that are necessary to maintain a PMR past 24 h by allowing Sex Peptide, the major trigger for the *Drosophila* PMR (30–32), to bind to and be stored with sperm (28, 33–39). Unfortunately, due to their

Significance

In many species, mating induces physiological changes in the female that increase the reproductive success of the mating pair. The postmating response (PMR) is caused by male seminal fluid proteins interacting with the female reproductive system. Because of the importance of the PMR in many insect species relevant to human health and agriculture, we examined the gene expression profile of one important cell type of the gland that produces most of the seminal fluid proteins in *Drosophila*. Interestingly, among proteins necessary for the PMR in this species, we discovered that a micropeptide encoded by a supposedly noncoding transcript is produced and carries out important reproductive functions. Such micropeptides were previously unrecognized but are emerging as important actors in complex biological processes.

Author contributions: C.I., M.F.W., F.K., and R.K.M. designed research; C.I., Y.F., S.Y.N.D., D.G., J.G., L.F., J.-C.B., and R.K.M. performed research; C.I., Y.F., S.Y.N.D., P.M.A., L.F., E.N., M.F.W., and R.K.M. analyzed data; C.I. and R.K.M. wrote the paper; and M.F.W. and F.K. supervised the research.

The authors declare no competing interest.

This article is a PNAS Direct Submission.

[1]Present address: Molecular, cellular and developmental biology (MCD) Unit, Centre de Biologie Intégrative, Université de Toulouse, CNRS, Bat 4R4, F-31062, Toulouse, France.

[2]To whom correspondence may be addressed. Email: clem.immarigeon@gmail.com or robert.maeda@unige.ch.

This article contains supporting information online at https://www.pnas.org/lookup/suppl/doi:10.1073/pnas.2001897118/-/DCSupplemental.

Published April 5, 2021.

scarcity (~40 SCs per gland), we still have a limited understanding of the functioning and genetic program of this important cell type. In the course of investigating SC function via two RNA sequencing-based approaches (based either on RNA abundance or association with ribosomes), we identified a noncoding RNA within the ribosome-bound population of transcripts. We confirm that this supposedly noncoding RNA, called *male-specific abdominal* (*msa*), contains a smORF that generates a 9- or 20-amino acid (aa) peptide, and that this peptide plays an important role in reproduction. *msa*, which is embedded within the HOX gene cluster of the Bithorax complex, was previously shown to be important for SC development and the PMR through the production of a miRNA (38). Here, we show that it is also the template for a conserved micropeptide that we call MSAmiP. Although MSAmiP is apparently dispensable for SC development and for the PMR, a precise deletion of this smORF elicits a sperm-competition phenotype in matings involving mutant males, showing that there may be many unannotated smORFs throughout the genome that play important biological functions.

Results

A Ribosome-Associated Noncoding Transcript Expressed in the Secondary Cells of the Accessory Gland. To identify the coding genes that make SCs essential to male reproductive success, we aimed to establish the transcriptome and the translatome of this rare cell population (Fig. 1 *A* and *B*). The SC transcriptome was determined using FACS-sorted SCs expressing GFP under the *AbdB*GAL4 driver (35) (SC>>GFP in Fig. 1*A*, procedure described in ref. 40). We used the TRAPseq technique (translating ribosome affinity purification-RNA sequencing) to define, among the RNAs detected in the transcriptome, the transcripts that are associated with ribosomes and thus potentially translated into proteins. TRAPseq can reveal the coding potential of transcripts annotated as noncoding (lncRNAs) and can also reveal that some canonical mRNAs are not actually translated in a particular cell type. This method has previously been used to characterize the translation of mRNAs by immunopurifying GFP-tagged ribosomes (41, 42). For this, we expressed either GFP alone ("mock" condition) or GFP-RPL10Ab tagged ribosomes ("TRAP" condition) specifically in SCs (Fig. 1*B*). We verified the specificity of the technique by showing that ribosomes and associated mRNAs from SCs but not from main cells were efficiently enriched in the TRAP compared to the mock condition (*SI Appendix*, Fig. S1). These datasets are accessible in Dataset S1. As shown in Fig. 1*C*, RNAseq and TRAPseq data are highly correlated (Pearson correlation coefficient ~0.9), which suggests that RNAseq generally gives a relatively accurate estimation of mRNA translation for most genes. However, TRAP is highly informative for specific genes that do not behave as expected, as exemplified by *Ubx* and *msa* (Fig. 1*C*). On one hand, the HOX gene *Ultrabithorax* (*Ubx*), is highly transcribed (21st most highly expressed RNA) but not translated in SCs (our TRAP data corroborate unsuccessful attempts to detect Ubx protein by immunostaining accessory glands) (38). On the other hand, *msa* is annotated as a lncRNA, but is associated with ribosomes, suggesting that it may encode unknown peptides.

Given the surprising finding of *msa* in our dataset, we sought to validate the accuracy and specificity of our screen by looking at the protein-coding genes. From the list of >7,000 genes robustly detected, we used a gating strategy to narrow the informative SC coding genes (see Fig. 1*D* for data analysis and cutoffs). After Gate#2, we obtained a list of 1,415 genes. Gene ontology using this gene list is consistent with secondary cell biology, as the most highly enriched terms are related to reproduction, postmating response, vesicle-mediated transport, secretion, and endocytosis, with many proteins predicted to be located at endomembranes, in vacuoles or in the extracellular space (Fig. 1*E*). This fits the current view of SCs as vacuole-filled secretory cells that produce, secrete, import, and modify proteins involved in the PMR. We then narrowed down the list of genes to the 151 transcripts that displayed the strongest transcription and ribosome association in secondary cells (Gate#3 genes, shown in red in Fig. 1*C*). These 151 genes include five of the six previously known SC markers *msa* (38), *Rab19* (27), *Dve* (39), *CG17575*, and *Lectin-46Ca* (27, 35), validating both procedures and data analysis (Dataset S2), and many encode secreted proteins that are associated with the PMR (regulation of female receptivity) and sperm competition (Fig. 1*E*).

Strikingly, a small number of RNAs make up the majority of transcripts (in terms of number of reads): the top seven genes contribute to >70% of all the transcriptome reads (Figs. 1*C* and 2*A*). Notably, these seven genes encode proteins known to be transferred to females during mating (43) (CG9029, Acp32CD, the CRISP CG17575, Lectin-46Cb, Lectin-46Ca, CG13965, and midline fasciclin/mfas), including two previously known to be expressed in SCs. Three of these genes [CG17575 (38), Lectin-46Cb, and Lectin-46Ca) (36, 37, 43, 44)] have already been characterized as regulators of the long-term PMR through transient binding to sperm (36, 37, 45), thus further validating the dataset as revealing important players in the SC's reproductive role. To extend this validation, we selected five uncharacterized genes among the most highly expressed SC transcripts (Fig. 2*A*) and assayed their function using standard PMR assays. We tested the ability of knockdown males to induce the decrease in female receptivity typically observed for many days after initial mating. We first tested CG9029, using two RNAi lines, as this was the most highly expressed gene and encodes a seminal fluid protein (43). While CG9029 was not required in SCs to initiate the PMR (no remating was observed at 24 h, not shown), we found that it is critical to extend the females' unreceptive nature past 1 d (Fig. 2*B*). Confirming the role of CG9029 in creating a long-term PMR, we also found that mates of knockdown males display lower levels of egg deposition at times after day 1 (*SI Appendix*, Fig. S2 *A* and *B*). The long-term PMR is mediated by Sex Peptide (32, 33, 46), which must be stored with the sperm to allow the PMR to last for more than 1 d. We thus tested if CG9029 affected Sex Peptide storage in the sperm storage organ. Upon SC knockdown of CG9029, Sex Peptide was undetectable by 24 h postmating (Fig. 2*C*). This explains, at a molecular level, why females are receptive to remating and lay fewer eggs after 1 d. We found analogous results for three of the other genes we tested: Acp32CD, CG31145, and GILT-3 (*SI Appendix*, Fig. S2 *C* and *D*), showing that these genes must be expressed in SCs to allow proper Sex Peptide storage and reduce female receptivity (26, 27, 47, 48). Of our five candidates, only CG13965 did not show a detectable long-term PMR phenotype.

Having validated our list of SC signature genes on the basis of scientific literature and experimental data for protein-coding genes, we were then confident to examine the supposedly noncoding transcript *msa* (38). Although this transcript is annotated as lncRNA, its detection at high levels in our TRAPseq led us to investigate its potential to encode previously unknown peptides.

The msa "lncRNA" Encodes SC-Specific Micropeptides. *msa* is a SC-specific isoform of the *iab-8 lncRNA* that spans the intergenic region between the HOX genes *Abd-B* and *abd-A* in the Bithorax complex (Fig. 3*A*). Previously, we showed that *msa* is critical for SC function (38) and that much of its function can be attributed to a miRNA, located within its fourth intron. As our data suggested that this transcript is also peptide-encoding, we verified our TRAP results using RT-qPCR on the ribosome immunopurified RNAs. Indeed, RT-qPCR confirms a strong enrichment of this transcript associated with SC ribosomes (*SI Appendix*, Fig. S1).

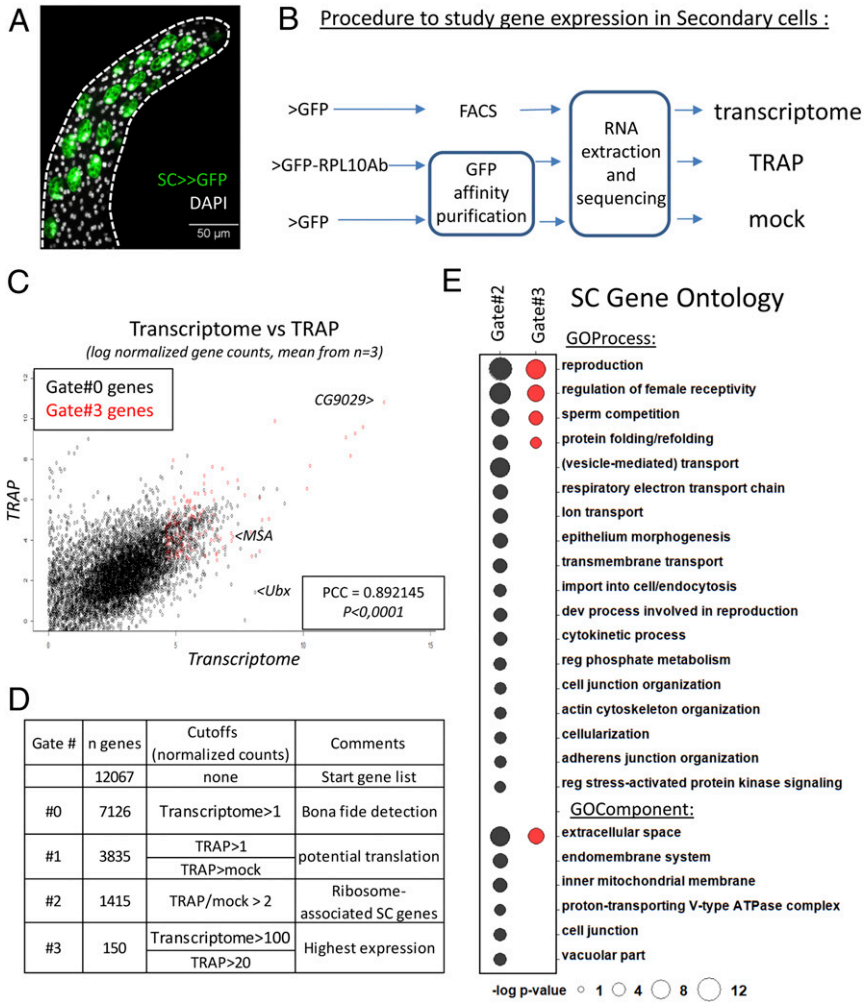

Gate #	n genes	Cutoffs (normalized counts)	Comments
	12067	none	Start gene list
#0	7126	Transcriptome>1	Bona fide detection
#1	3835	TRAP>1 TRAP>mock	potential translation
#2	1415	TRAP/mock > 2	Ribosome-associated SC genes
#3	150	Transcriptome>100 TRAP>20	Highest expression

Fig. 1. Transciptome and TRAPseq analysis highlight secondary cell functions. (*A*) The ~40 secondary cells (SCs, expressing GFP) are visible at the distal tip of the *Drosophila* male accessory glands (outlined with a dashed line), surrounded by main cells. SCs display large vacuole-like structures (GFP-negative) and are binucleated. DAPI staining is shown in gray. This confocal Z stack shows the cells on one side of the glandular lumen. (Scale bar, 50 µm.) (*B*) Our strategy to identify SC coding genes. Using a SC-specific Gal4 driver (SC>), we expressed either >GFP alone or a GFP-tagged ribosomal subunit (GFP-RPL10Ab). GFP-expressing secondary cells were sorted (fluorescence-activated cell sorting, FACS) and their RNA were sequenced to establish SC transcriptome. Affinity purification of GFP was performed and associated RNAs were sequenced to establish SC TRAPseq and mock control. (*C*) Scatterplot showing gene counts in transcriptome and TRAP data. For each gene, the mean normalized counts from three replicates is plotted on a logarithmic scale. PCC, Pearson correlation coefficient. *P* value <0.0001. Gate#3 genes are shown in red (see *D*). (*D*) Gating strategy to find SC signature-coding genes from our normalized sequencing data (Dataset S1). For each Gate, the cutoff above which genes are kept is indicated, together with a comment about the rationale for it and the number of remaining genes. (*E*) Gene ontology (GO) of secondary cells using Gate#2 (black) and Gate#3 (red) genelists as input in http://cbl-gorilla.cs.technion.ac.il/ (genes ranked following transcriptome counts). Synonymous and noninformative terms were removed for clarity. An exhaustive list of GO terms is available upon request.

This RNA contains a block of sequence located within its last exon that we previously identified based on its conservation in several *Drosophila* species (49). This block starts with an ATG and finishes with two, in-frame, putative stop codons and could encode a 9-amino acid peptide. As this analysis was based on a limited number of species, we extended the prior evolutionary analysis to more *Drosophila* species (Fig. 3*B* and Dataset S3). This revealed that the block of sequence conservation extends to another upstream ATG. We also note sharp drops in conservation both upstream of the first ATG (M) and downstream of the stop codons (*), as evidenced by the "amino-acid conservation" plot and DNA sequence consensus line in Fig. 3*B*. Thus, the conserved region consists of a putative smORF with up to three in-frame ATGs that could code for overlapping small peptides of 20, 9, or 3 amino acids, respectively. Although we could not find any convincing homologs outside of the *Drosophila* genus, we find this sequence in Drosophilidae from multiple subgenera (Fig. 3*B* and Dataset S3). This sequence has thus been conserved for over 60 million years of evolution (the last common ancestor of *D. melanogaster* and *Drosophila willistoni* has been estimated to have lived 62.2 Mya) (50). We call this multi-ATG putative smORF "*MSAmiP* smORF" (*msa* micropeptide small open reading frame), and will refer to the encoded peptides as MSAmiP20, MSAmiP9, and MSAmiP3 depending on their size in amino acids.

Conservation of the putative *MSAmiP* smORF shows that the amino acid sequence of MSAmiP9 has mostly been unchanged in all the species tested, with most mutations being silent or conservative (e.g., L to F, Fig. 3*B*). The MSAmiP20 sequence, by comparison has accumulated more mutations, as exemplified for *Drosophila busckii* whose MSAmiP20 is the most divergent with 6/20 amino acid changes. However, protein structure prediction

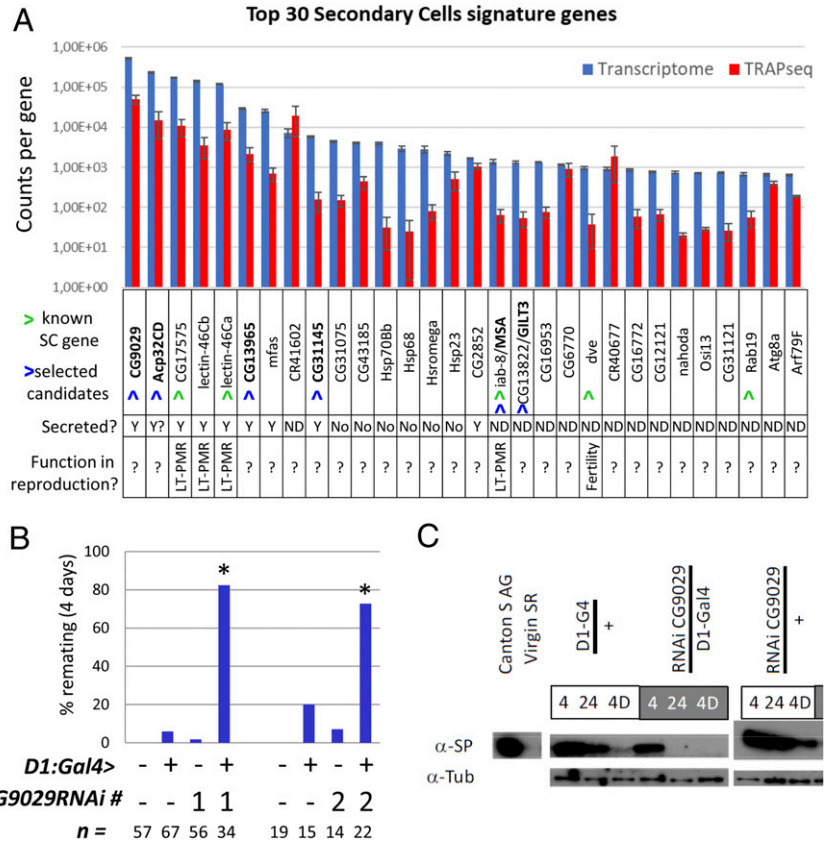

Fig. 2. Secondary cell signature genes contain unstudied yet important genes. (*A*) Top 30 SC signature genes are ranked according to their RNA expression level as normalized counts per gene (in blue). The TRAPseq count for each gene is shown in red. Error bars show the SDs ($n = 3$). Green arrowheads highlight known SC genes and blue ones highlight the candidates we selected for functional investigation. Additional information for each gene is indicated below the graph. Y, yes; LT-PMR, long-term PMR. (*B*) Four-day receptivity assays on *Canton S* females mated individually with male flies of the genotypes listed below the graphs. Remating was scored for 1 h. CG9029 was specifically knocked down in SCs using the GAL4-UAS system (78), with the help of two different UAS-RNAi lines to circumvent potential off-target effects. The * highlight the significant differences. Number of individual mated females is given as "*n* =." (*C*) Western blot analysis of Sex Peptide (SP) storage in female seminal receptacles (SRs) at different time points after mating with males depleted for CG9029 in the SCs. 4 = 4 h postmating, 24 = 24 h post mating, 4D = 4 d postmating.

software (PEP-FOLD 3.5) suggests a helical conformation for the MSAmiP9 portion, which is retained in the analysis of the MSAmiP20 sequences. This predicted structural conservation suggests that selective pressure may have occurred at the protein level and could indicate that the MSAmiP-encoded peptides are functional.

To investigate the translation potential and function of this smORF in vivo, we generated genetic tools to modify its endogenous sequence within the Bithorax complex (Fig. 3*A*). Using CRISPR-mediated cassette exchange, we replaced the exon of *msa* containing the putative smORF with a site-specific integration platform (attP) (51). Using this "*Δexon8 attP*" platform, we could then insert any modified version of the exon into its normal genomic locus via PhiC31-mediated recombination: we generated a rescue construct (*exon8wt rescue*), a clean *MSAmiP* smORF knockout (*ΔMSAmiP*), and a C-terminal GFP fusion construct (*MSAmiP-GFP*). Note that the GFP portion of the *MSAmiP-GFP* fusion lacks its start codon to prevent GFP translation independent of the smORF. Examination of the *MSAmiP-GFP* flies revealed GFP expression in the SCs (Fig. 3*C*), confirming that *msa* encodes at least one small peptide translated from this *MSAmiP* smORF. GFP expression from MSAmiP-GFP seems to accumulate in SC nuclei (as revealed by colocalization with DAPI staining) (Fig. 3 *C′* and *C′′*) but some was also observed in the cytoplasm where it was excluded from the large vacuoles. As GFP signal was not seen elsewhere in any of the other tissues examined at any developmental stages, we conclude that *MSAmiP* is only translated in the SCs.

MSAmiP Mutant Males Have Increased Sperm Competition Defensive Abilities. To investigate MSAmiP function without affecting the other functions of *msa* (e.g., *miR-iab-8*), we compared the *ΔMSAmiP* line, in which the 60 base pairs of the *MSAmiP* smORF are deleted, to the *exon8wt rescue* line (control), in which the intact *exon8* was placed back at its normal location (Fig. 3*A*). These two lines contain virtually identical genomes, except for the presence or absence of the *MSAmiP* smORF. Previously, we showed that a deletion of the promoter of *msa* results in phenotypes affecting fertility, maintenance of the PMR, and sperm competition (35). To test if any of these phenotypes can be attributed to the loss of MSAmiP, we tested *ΔMSAmiP* males for their ability to mediate these processes. We first tested fertility and the PMR. Upon single mating, *MSAmiP*-deficient males produce as many offspring as control males (*SI Appendix*, Fig. S4*A*). After 4 d, females mated to these males were tested for receptivity to courting males. In this assay, *ΔMSAmiP* mated females are unreceptive to remating at 4 d, similar to females mated to control males (*SI Appendix*, Fig. S4*B*). Based on these assays, we conclude that MSAmiP is not involved in fecundity or in triggering the PMR.

We then tested *ΔMSAmiP* males to see if the mutant recapitulated the sperm-competition phenotype that we had previously

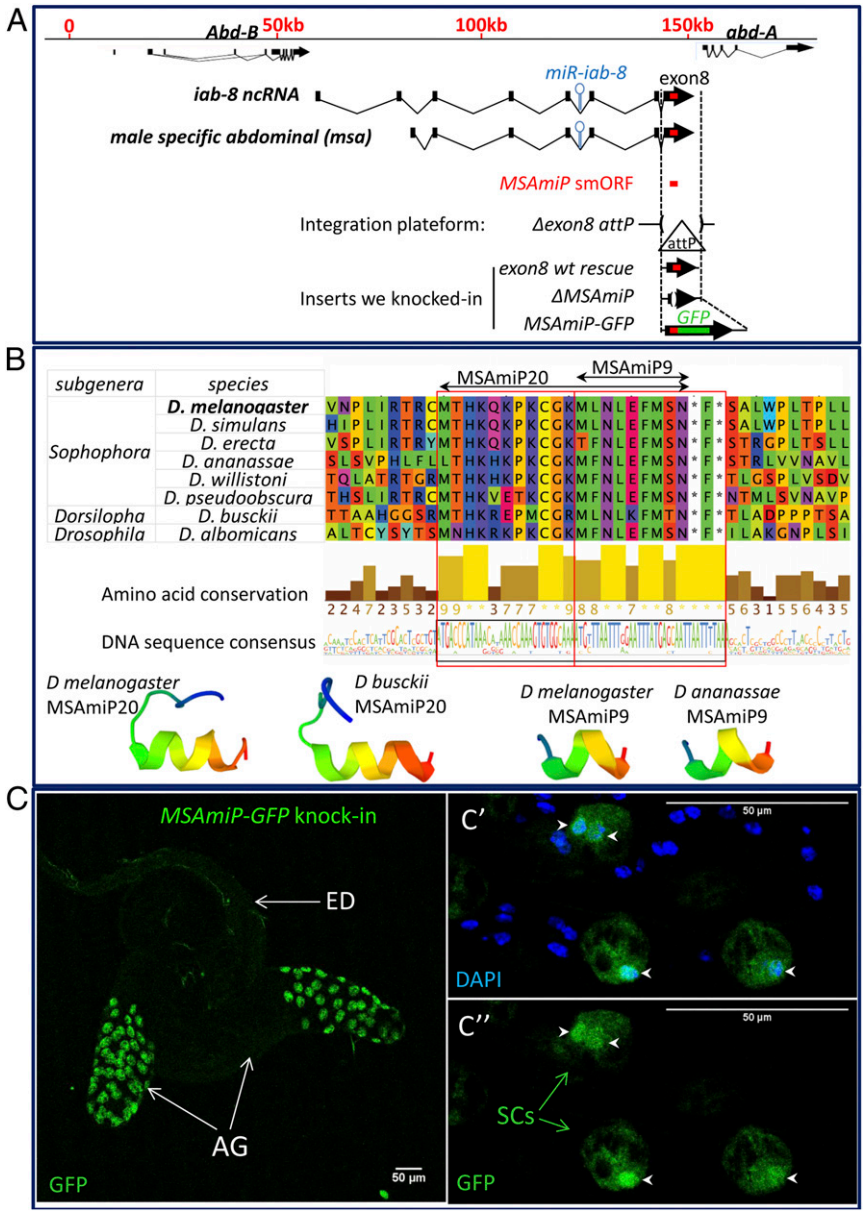

Fig. 3. *MSAmiP* smORF is conserved and encodes a micropeptide translated in SCs. (*A*) The top line represents the abdominal region of the Bithorax complex marked off in kilobases, with the structure of the *Abd-B* and *abd-A* transcription units. The structures of the *iab-8 ncRNA* and *msa* are drawn below. Exons are indicated as black boxes (not to scale). Arrows represent the last exon and the sense of transcription. The blue hairpin shows the approximate location of *miR iab8*. The *MSAmiP* smORF is indicated in red in the last exon (exon8) of the msa *RNA* and of the *iab-8 ncRNA*. Note that the *msa* RNA originates from an alternative promoter (active only in SCs) and shares all its downstream exons with the 3′ exons of the the *iab8 ncRNA*. The genetic tools generated to study *MSAmiP* smORF are presented below. Dotted vertical lines show the limits of the CRISPR-mediated deletion (*Δexon8*) where exon8 is replaced by an *attP* integration site. This *Δexon8 attP* platform was used to generate several modifications of the endogenous locus, including *exon8 wt rescue*, *ΔMSAmiP* deletion, and *MSAmiP-GFP knockin* (green rectangle represents GFP ORF fused to *MSAmiP* smORF). (*B*) *MSAmiP* smORF conservation among *Drosophilidae*. Amino acid sequence alignment of the genomic region surrounding MSAmiP smORF in *Drosophila* species from multiple subgenera shows that the conserved block starts at MSAmiP20 methionine (M) and stops after the stop codons (*). Level of each amino acid conservation is represented underneath as a barchart (Jalview 2.10.5 version (http://www.jalview.org/) using clustalx coloring. Structure predictions using PEP-FOLD 3.5 show that resulting polypeptides could adopt very similar tridimensional conformations with helical C terminus. (*C*) *MSAmiP* is translated in secondary cells. The genital tract from a *MSAmiP-GFP* knockin male is imaged live (no fixation or staining) and GFP is visible in SCs. AG, accessory glands; SCs, secondary cells; ED, ejaculatory duct. (Scale bars, 50 µm.) *C′* and *C′′* show GFP accumulation in SC nuclei (stained with DAPI, arrowheads), in fixed tissue.

observed for males lacking the *msa* transcript (35). Generally, if a *Drosophila* female mates with two males, the second male will sire most of the progeny ("last male sperm precedence") (52–55); the first male's sperm are displaced by those of the second male (56–59). Previously, we had shown that if the first male lacked *msa*, last male precedence was reduced (35). To test the role of MSAmiP in this phenomenon, we used the assay schematized in Fig. 4*A* to score the relative proportion of progeny sired by two different males successively mated to a female. Fig. 4*B* shows the result from *ΔMSAmiP* and control males. As expected, in the control condition there is a strong preference for the sperm from the last male (mean P1 = 0.26 for *exon8wt rescue*). In contrast, when the first male lacks MSAmiP, last male precedence is greatly reduced (mean P1 = 0.45). Importantly, the total number of

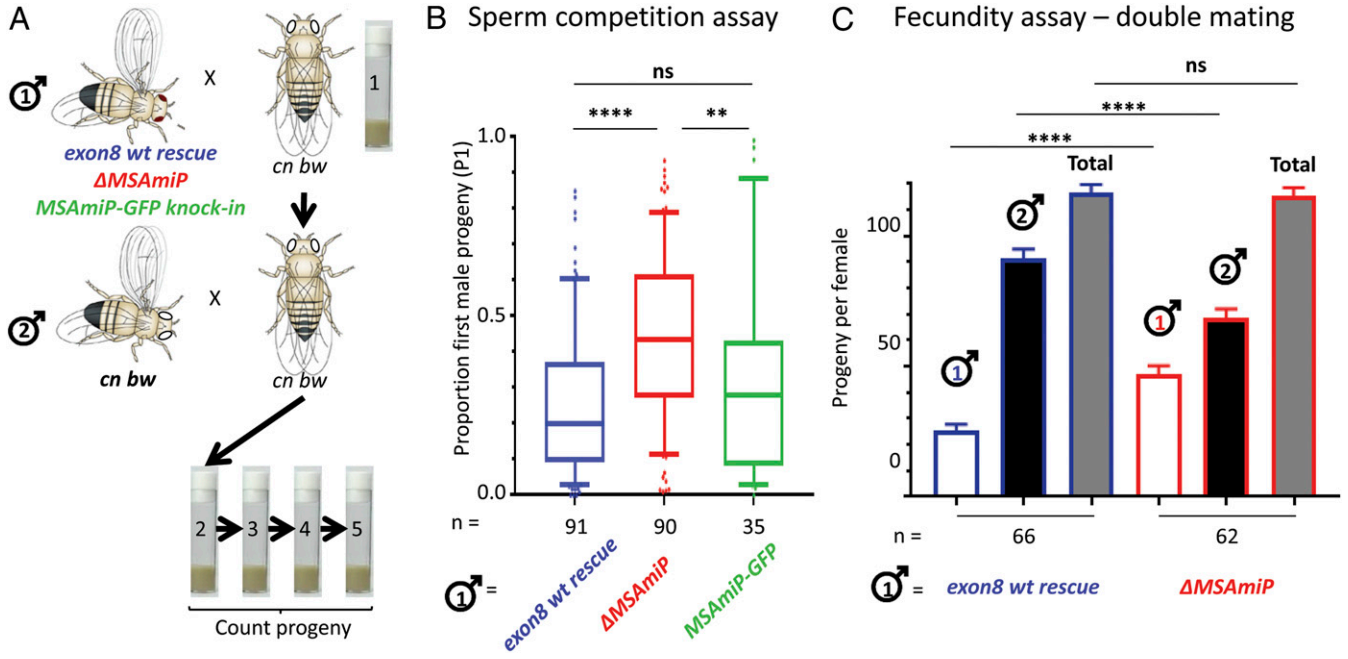

Fig. 4. *MSAmiP* is involved in sperm competition. (*A*) Experimental setup to test the sperm-competition defensive ability of the three mutant males indicated in blue, red, and green. Individual *cn bw* females with white eyes are crossed first to a red-eyed male (test male 1) and then remated to white-eyed males (*cn bw* male 2). Eggs are collected over 8 d in four successive vials. Paternity is scored based on offspring eye color. (*B*) Proportion of the progeny sired by male 1 (P1) depends on MSAmiP. Results are shown as box and whiskers plots showing 10 to 90 percentile and the median. A *P* value of <0.0001 (****) was observed for *ΔMSAmiP* mutant vs. *exon8 wt rescue.* For *exon8 wt rescue* vs. *MSAmiP-GFP knockin*, the *P* value was 0.9 (not significant, ns). Finally the *P* value for *ΔMSAmiP* mutant vs. *MSAmiP-GFP knockin* was 0.0065 (**). Number of individual, doubly mated females is given (*n* =). See *Materials and Methods* for statistical analysis. (*C*) The number of progeny sired by males 1 and 2. Statistical tests are similar to previous ones but assuming a Poisson distribution. The total number of offspring is not affected by the genotype of the first male (ns, $P = 0.9187$), but the respective progeny of each male is significantly affected ($P < 0.0001$ for both comparisons).

progeny from each female is not affected (Fig. 4*C*, gray bars) but the proportion of progeny from each male changes (Fig. 4*C*, white and black bars). Thus, we conclude that the sperm-competition phenotype observed in males lacking *msa* (*iab-6*^{cocuD1} mutants) (35) is likely due to the loss of MSAmiP and is related to sperm storage/usage by the female in a competitive context, and not due to a fecundity issue. Interestingly, the relative success of *MSAmiP-GFP* knockin males is similar to that of control *exon8wt rescue* males, indicating that the MSAmiP-GFP fusion is functional (Fig. 4*B*).

Given the subtlety of the sperm-competition phenotype and the fact that the *ΔMSAmiP* and *exon8wt rescue* lines differ by 60 base pairs, it was important to confirm that the sperm-competition phenotype observed with *ΔMSAmiP* males is due to the loss of the micropeptide rather than to the loss of an enhancer sequence present within this interval or to destabilization of the *msa* RNA. The latter options were ruled out by transcriptome analysis of flies carrying the *ΔMSAmiP* deletion, which showed that this mutation does not destabilize the *msa* transcript (*SI Appendix*, Fig. S3*A*), or remove critical *cis*-regulatory elements required for expression of any genes nearby (*SI Appendix*, Fig. S3*B*). To confirm directly that the sperm-competition phenotype results from the loss of MSAmiP peptides, we assayed a frameshift mutant of *MSAmiP-GFP* in which only a single nucleotide was removed (*MSAmiP*3-GFP*, schematized in Fig. 5*A*). We observed that *MSAmiP*3-GFP* mutant males also display a significantly higher P1 ratio than *MSAmiP-GFP* controls (*SI Appendix*, Fig. S4*C*). These results verify that MSAmiP smORF-encoded peptides are likely responsible for the sperm-competition phenotype.

MSAmiP Seems to Primarily Be a 9 Amino Acid Micropeptide That Accumulates in SC Nuclei. The *MSAmiP* smORF contains three in-frame ATG initiation codons that could initiate translation of three different polypeptides (Fig. 3*B*). To determine the relative contribution of each ATG to translation, we cloned the cDNA of *msa* and placed the *GFP* sequence downstream of the *MSAmiP* smORF. When expressed in cultured cells, this construct elicits strong fluorescence. From this construct, we generated a series of derivatives containing frameshift mutations after each putative start codon: fs1 downstream of the MSAmiP20 ATG, fs2 downstream of the MSAmiP9 ATG, and fs3 downstream of the MSAmiP3 ATG (*SI Appendix*, Fig. S5*A*). While these modifications should selectively prevent GFP fluorescence from translation events initiating upstream of the frameshift, they should not interfere with translation initiation itself, thus giving a relative estimate of the amount of GFP originating from each ATG. We quantified GFP fluorescence in fixed cells expressing one of the *msa cDNA-MSAmiP-GFP* constructs, and observed that fs1 did not affect GFP intensity, while fs2 and fs3 caused a drastic decrease in GFP fluorescence (*SI Appendix*, Fig. S5*B*). Based on these experiments, MSAmiP9 appears as the most abundant isoform.

We then took advantage of our *Δexon8 attP* integration platform (Fig. 3*A*) to ask the same question in living flies. We knocked in three modified versions of *MSAmiP-GFP* which can only produce one isoform of MSAmiP fused with GFP. These fly lines are called MSAmiP*3-GFP, MSAmiP*9-GFP, and MSAmiP*20-GFP (Fig. 5*A*). As a control for artifactual GFP translation, independent of the *MSAmiP* smORF, we generated the "*Frameshifted MSAmiP-GFP*" (*fs-MSAmiP-GFP*) line that cannot initiate translation of fluorescent GFP from any of *MSAmiP* ATGs. As shown in Fig. 5*B*, most of the GFP signal from the MSAmiP-GFP knockin can be attributed to the MSAmiP9 ATG, which elicits more fluorescence than the other lines. This result can also be seen on Western blots of knockin male accessory glands using an antibody against GFP (Fig. 5*C*). Notably, both MSAmiP*3-GFP and MSAmiP*20-GFP produce weak fluorescence in SCs, and

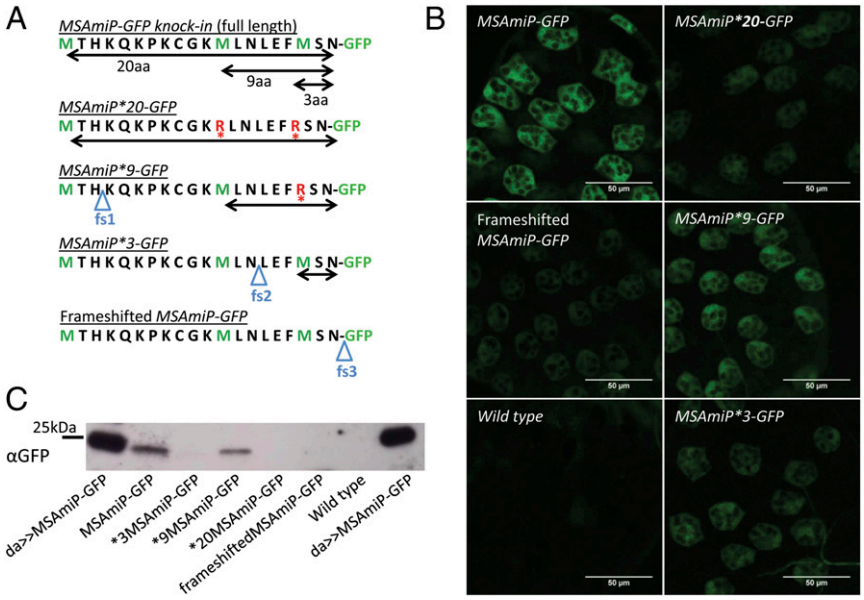

Fig. 5. MSAmiP9 seems to be the most abundant peptide encoded by *msa* in vivo. (*A*) Design of the isoform-specific MSAmiP-GFP* knockins. The amino acid sequence encoded by *MSAmiP* smORF is shown with methionines highlighted in green (M). Horizontal double arrows represent the different MSAmiP isoforms that may produce a GFP fusion in each construct. Blue triangles labeled fs show the position of the frameshift mutations, and red asterisks show point mutations of methionine-into arginine-codon (R). (*B*) Confocal image (Z slice) of a live AG distal tip representative of each genotype. (*C*) GFP fusion protein detected by Western blot from male accessory glands.

MSAmiP*9-GFP alone does not elicit as much fluorescence as the full-length knockin. Thus, our results using both tissue culture cells and fly accessory glands suggest that the 9 amino acid form of MSAmiP is the predominant form of the peptide (Fig. 5 *B* and *C* and *SI Appendix*, Fig. S5). However, other isoforms are probably produced at lower levels.

Upon examining the localization of MSAmiP-GFP, we found that GFP signal was largely enriched in SC nuclei with some cytoplasmic staining, but no signal in the large vacuoles (Fig. 3*C*). This staining is restricted to SCs. Although MSAmiP-GFP is functional according to our sperm-competition assay (Fig. 4*B*), we worried that the subcellular localization could be partially artifactual due to the GFP tag, which has been shown to accumulate in the nucleus (60). Because our attempts to make specific antibodies to MSAmiP were unsuccessful, we confirmed the subcellular localization of MSAmiP using a different tag. For this, we generated an N- and C-terminal Flag-HA-tagged version of MSAmiP (FLAG-HA-MSAmiP20 and MSAmiP-Flag-HA). Note that for the N-terminal-tagged version we used the miP20 methionine as the start codon. Although miP20 does not seem to be the most abundant form of MSAmiP, it does seem to be expressed and we reasoned that its localization might be less affected by the addition of a tag. For both tagged constructs, we observed accumulation of signal in SC nuclei (Fig. 6, see the

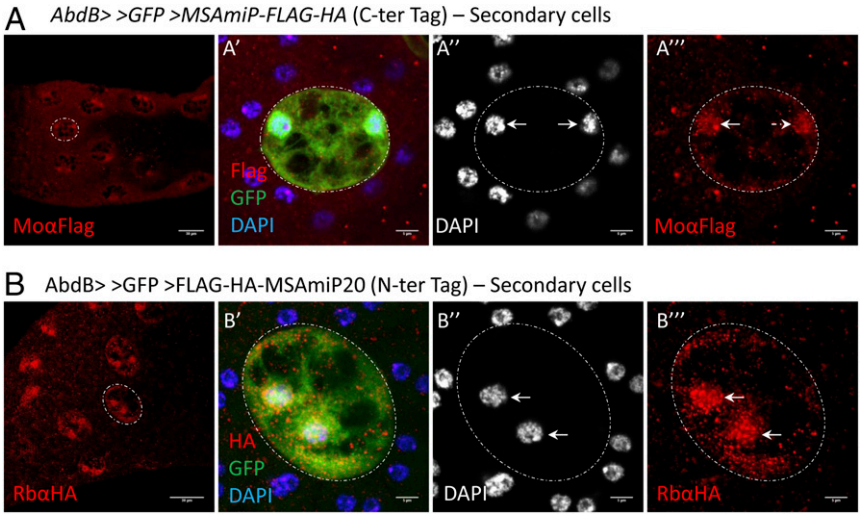

Fig. 6. MSAmiP localizes preferentially to secondary cell nuclei. Confocal image (1z) of male accessory glands expressing GFP and MSAmiP-FLAG-HA (*A*) or FLAG-HA-MSAmiP20 (*B*) in secondary cells. Close-up of a single SC is shown with its contours indicated by the dashed lines. GFP is in green (*A*′ and *B*′), DAPI in blue (*A*′ and *B*′) or gray (*A*′′ and *B*′′), and Flag (*A*, *A*′, and *A*′′′) or HA (*B*, *B*′, and *B*′′′) in red. While most of the MSAmiP-FLAG-HA/Flag-HA-MSAmiP20 signal is seen in nuclei, a weak signal is also visible in the cytoplasm. (Scale bars in *A* and *B*, 30 μm; 5 μm in close-ups.)

close-ups on individual, binucleate SCs). Furthermore, this result could be confirmed in cultured cells (*SI Appendix*, Fig. S6), suggesting that the nuclear enrichment is an intrinsic property of MSAmiP.

Discussion

MSAmiP, a Micropeptide Required for Proper Sperm Competition. The data presented in this study show that the *msa* transcript, annotated as a lncRNA, encodes a micropeptide involved in sperm competition. We previously reported a similar sperm-competition phenotype for the *iab-6*^{cocuD1} mutant using the same assay shown in Fig. 4 (35). Subsequently, we showed that the *iab-6*^{cocuD1} mutant was a deletion of a region (the *D1* enhancer) that includes the *msa* promoter, and that several *iab-6*^{cocuD1} mutant phenotypes were attributable to *msa*, and in particular to *miR-iab-8*, a micro-RNA nested in one of the introns of *msa* (38). So far, the loss of MSAmiP is the only clearly documented reason for the *iab-6*^{cocuD1} mutant phenotype in sperm competition.

Here, we find that *ΔMSAmiP* males sire a larger proportion of offspring than the wild-type control, when it is the first male to mate in a sperm-competitive situation. This initially seems counterintuitive, as one might think that the relative competitive success of males without *MSAmiP* might have led to the loss of the peptide-coding sequence due to selection. However, the surprising phenomenon of a deficient male doing better as first male has been seen in mutants for a number of seminal protein genes or secondary cell regulators: Sex Peptide, ACP62F, and Dad (BMP signaling); as with ΔMSAmiP, loss of function of these genes enhanced sperm defensive ability in sperm-competition assays (56, 61–63). A potential explanation for these results is based on findings with Sex Peptide and Dad. Their increased sperm defensive ability appears to be a consequence of inefficient release of the mutant male's sperm from its storage in the female: both Sex Peptide and Dad mutant sperm are overretained in the sperm storage organs (48, 56). Thus, there are more of them left to compete with the second male's sperm when second mating occurs. In light of these and recent data (64), we propose that while overretention of sperm (such as those from *ΔMSAmiP* males) in storage organ may enhance success in sperm-competition assays, the failure to properly release those sperm in the first place may be detrimental to the male's production of offspring over time, and hence the genes are not lost during evolution.

How MSAmiP mediates its function remains unclear. Our data show that MSAmiP accumulates in SC nuclei (Figs. 3*D* and 5), which suggests that it could play a role in gene expression. However, examination of the *ΔMSAmiP* SC transcriptome reveals little difference compared to wild-type cells (*SI Appendix*, Fig. S3), with only six genes significantly misexpressed (CG9119, ppk20, CG13360, CG33080, nSyb, and CG7582, see Dataset S4 and *Materials and Methods* for statistical analysis). None of these genes point to an obvious explanation for the phenotype we observed, nor to additional phenotypes to explore. Importantly, none is significantly misexpressed in the same direction in the *iab-6*^{cocuD1} (*msa* mutant) transcriptome (Dataset S1), so we consider it unlikely that these genes are the functionally relevant MSAmiP targets. Thus, based on our statistical analysis of differentially expressed genes, we conclude that the effect of MSAmiP expression is subtle and does not dramatically affect transcript levels in SCs.

Based on our GFP fusion data, MSAmiP seems to predominantly be a 9-amino acid peptide with some additional expression coming from other in-frame ATG(s) (Fig. 5). Examining the peptide sequence in different *Drosophila* species, we can see that depending on the species, the 9-amino acid methionine or the 20-amino acid methionine has been lost (see *Drosophila erecta* and *Drosophila ananassae* in Fig. 3*B*). This could indicate that both forms are functional. Although we favor a model in which the 9-amino acid form is more abundant in *D. melanogaster*, we do see the 20-amino acid form expressed at a noticeable level (Fig. 5) and we cannot rule out the possibility that our mutations change the usage ratio of each methionine of the peptide stability. Regardless of the exact size, MSAmiP is a small peptide. Thus, like other micropeptides (16, 18) MSAmiP would probably need to interact with other factors to be biologically active. As our GFP fusion protein seems to be functional (Fig. 4*B*), it could provide a useful tool to search for binding partners.

smORF-Encoded Peptides Should Receive More Attention. Our findings with MSAmiP provide a strong argument for the consideration of smORFs as a source of biologically significant molecules. A growing number of such peptides are now known to be involved in the development of cancers and are being investigated as potential tumor markers, therapeutic targets, or drugs (65). Interestingly, one of these peptides is produced from a transcript annotated as a lncRNA from the human HOX B cluster and has been shown to suppress colon cancer growth (66). Like MSAmiP, this peptide was found through a combination of transcriptome and translatome methods. Although these peptides show no identifiable similarity at the sequence level, the finding of two peptides expressed from Hox gene complexes in two distant organisms is of note and may indicate that the Hox complexes are somehow an evolutionary environment conducive to the appearance/retention of smORFs. Alternatively, and perhaps more probably, this finding may simply reflect the vast underestimation of the number of functional peptides stemming from smORFs in eukaryotic genomes.

In line with this, five other SC signature genes in our dataset are annotated as ncRNAs: *Hsromega*, *CR40963*, *CR42862*, *CR41602*, and *CR40677* (Dataset S2). Interestingly, *Hrsomega* encodes a conserved 27-aa peptide that is translated upon stress induction and has been shown to be associated with translating ribosomes (67). Although it remains to be determined why *CR40963* and *CR42862* are associated with ribosomes, it seems very possible, based on our data, that they may code for novel small peptides. *CR41602* and *CR40677* are annotated as ribosomal RNA pseudogenes. Thus, their high TRAPseq counts may simply reflect the integration of these RNAs into the purified ribosomes and not their translation potential (like our 18S rRNA TRAP-qPCR control, *SI Appendix*, Fig. S1*A*).

Genomic Insights into the Translatome of an Important Secretory Cell Type. Secondary cells of *Drosophila* male accessory glands play a critical role in reproduction (27, 28, 35, 38, 39), but the nature of their products, and the function of those molecules is not yet well understood. Here, we shed light on this rare cell population, using transcriptome and TRAPseq analysis as an entry point. We find that SCs are highly specialized cells, whose most abundantly translated RNAs encode proteins necessary for the long-term PMR: the top seven SC signature-coding genes represent more than 70% of total transcriptome reads, and encode secreted proteins critical for the long-term PMR (Fig. 2 and *SI Appendix*, Fig. S2). In addition, our transcriptomics analysis of SC reveals an enrichment for GO terms related to import and endocytosis (Fig. 1*E*). SCs might thus import proteins from neighboring main cells and use their unique network of vacuole-like structures (27) to modify them posttranslationally, prior to secretion into the lumen.

Interestingly, our data revealed some surprises about the relative transcription and translation of RNAs in these cells. Although highly transcribed genes are expected to produce large amounts of protein and lncRNAs are not, comparing the transcriptome and TRAPseq of SCs shows that these assumptions can be wrong. The *Ubx* (*Ultrabithorax*) mRNA is highly represented in the SC transcriptome (21st most highly expressed gene), yet it appears to be untranslated in SCs (Dataset S1 and Fig. 1*C*), confirming results obtained by the immunostaining of accessory glands (38). Conversely, the *msa* transcript has long

been annotated as a lncRNA but our TRAPseq showed that it was ribosome-associated, and our further analysis reported here shows that it encodes a micropeptide in SCs. These findings highlight the importance of examining both translatome and transcriptome data before the selection of potential functional candidates.

At the other end of the lncRNA spectrum, some lncRNAs may play a role in SC biology through their RNAs. For example, microRNA precursor *CR43314* and *iab-4* are expressed (but not translated) in SCs (Dataset S1) and probably play a role in the posttranscriptional regulation of gene expression. Notably, *miR-iab-4* is the complementary miRNA to *miR-iab-8* made by *msa*, and both of these miRNAs target *Ubx* (68–72), possibly responsible for the *Ubx* mRNA being untranslated in SCs.

Newly Characterized SC Genes Can Help Uncouple the Sequence of Events Leading to the Long-Term PMR. In addition to discovering that a micropeptide is translated and important in SC function, our transcriptome studies identified SC signature-coding genes (Dataset S2 and Fig. 2), including some with known function and expression (verifying our screen) and several for which we found reproductive function. Interestingly, SC genes appear to be involved at different steps of the cascade of events leading to the long-term PMR, confirming that an important role of SCs is to lengthen the PMR through the storage of Sex Peptide (Fig. 2*C* and *SI Appendix*, Fig. S2).

Notably, three of the five most-expressed SC genes (*CG17575*, *Lectin-46Cb*, and *Lectin-46Ca*) belong to the previously known network of accessory gland proteins that allow Sex Peptide to bind to sperm for storage (36, 37, 43, 44). However, these proteins bind sperm only transiently, and hence are not the actual scaffold on which Sex Peptide anchors (36). Here we show that additional proteins secreted by SCs are also critical for Sex Peptide storage past 1 d (CG9029, ACP32CD, and CG31145) and thus represent candidate scaffold proteins, or sperm modifiers that allow Sex Peptide binding. For example, CG9029 sequence does not show strict homology to proteins with known functions; it is predicted to encode a protein of 122 aa, high in mucin-like, O-linked glycosylation sites (S/T rich PxP repeats). As mucin proteins form polymers and biofilms, this might be consistent with a scaffolding role.

Concluding Remarks. In this study we used transcriptome and TRAPseq as entry points to study secondary cells (SCs), a rare secretory cell type. In addition to gaining insights into SCs' products and functions, we made a surprising discovery: a transcript classified as noncoding from the Bithorax HOX gene cluster was found to code for a set of small peptides that we call MSAmiP. These peptides, produced specifically in a few cells, affect male reproductive success, and have been conserved through *Drosophila* evolution. MSAmiP is a peptide produced from an miRNA precursor transcript in animals. This study shows that small peptides, including ones encoded by RNAs previously designated as ncRNA, are a potential reservoir of novel functional proteins, whose importance may only manifest in specialized cell types.

Materials and Methods

Plasmid and Transgenic Fly Line Generation. Cloning strategies to generate all plasmids used in this study are detailed in *SI Appendix*. The successive steps to obtain the *Δexon8 attP* platform using CRISPR, followed by PhiC31 site-specific integrations to obtain the multiple knock-in lines and the ΔMSAmiP are described in *SI Appendix*. See Dataset S5 for PCR primers, Gblocks, and CRISPR guides.

Secondary Cell Transcriptomics and TRAPseq. SC sorting and transcriptome are described in detail in ref. 40. TRAPseq was performed following the protocol from ref. 41, with adaptations detailed in *SI Appendix*. Briefly, for each biological replicate (n = 3) 250 male genital tracts expressing GFP-Rpl10Ab (TRAP) or GFP (mock) in SCs were recovered, lysed, and submitted to anti-GFP immunoprecipitation. RNAs were extracted and polyA+ RNAs were sequenced. Sequencing procedure, gene counts, and data analysis are detailed in *SI Appendix*.

Fly Stocks. To sort SCs by FACS, *UAS-GFP* expression was driven in SCs using *AbdB:Gal4* and *D1:GAL4* (35, 38) and the *iab-6*^{cocuD1} mutant (35). For TRAP UAS GFP-RPL10Ab (41) recombined with *D1:GAL4* was used. *UAS-RNAi* lines to test new candidate genes were obtained from the TRiP collection and VDRC (Vienna Drosophila Resource Center) collections: *CG9029* RNAi1 = *TRiP HMJ22752* and RNAi2 = *TRiP HMS02425*; *GILT3* RNAi1 = *102104KK* and RNAi2 = *38069GD*; *CG13965* RNAi1 = *41223GD* and RNAi2 = *106357KK*; *CG31145* RNAi1 = *108878KK* and RNAi2 = *25036GD*; and *Acp32CD* RNAi1 = *102687KK*. All transgenic lines generated in this study are detailed in *SI Appendix*.

Antibodies. Antibodies used in the course of this study include: rabbit anti-GFP (Torrey Pines), mouse anti-Flag M2 (Sigma), rabbit anti-Sex Peptide (32), goat anti-rabbit-HRP (horseradish peroxidase coupled antibody, Promega), rat anti-tubulin (ab6160, Abcam), and sheep anti-rat-HRP (ab6852, Abcam).

Microscopy and GFP Fluorescence Quantification. Micrographs used in this study were acquired using a Leica SP8 confocal microscope (Figs. 1, 3, 5, and 6) or a regular fluorescence/phase contrast microscope (*SI Appendix*, Fig. S2 *E* and *F*). *MSAmiP-GFP* knockin images are taken from unstained, freshly dissected live glands. Images from Figs. 1 and 3*C* and *SI Appendix*, Fig. S6 are maximal projection of multiple confocal Z (stack). Images in Figs. 3 *C′* and *C″*, 5, and 6 are single Z images. The procedure to obtain quantifications shown in *SI Appendix*, Fig. S5 is detailed in *SI Appendix*.

Western Blots. All detail can be found in *SI Appendix*. Briefly, for Fig. 2*C* and *SI Appendix*, Fig. S2*D*, single pair matings were performed and the mated females were snap frozen in liquid nitrogen after 2 to 4 h, 24 h, or 4 d after mating. The equivalent of approximately five female seminal receptacles were run per well. For Fig. 5C: five pairs of accessory glands from 1-d-old males are loaded for each knockin and wild-type lane and one pair of glands is loaded for the *da>>MSAmiP-GFP* positive control (*daughterless:GAL4 > UAS:MSAmiP-GFP*).

Receptivity Assays. We set up single pair matings in vials at room temperature using 5-d-old virgin *Canton S* females and 5-d-old tester males. Males were removed after copulation ended. Females were left in the vial and after 4 d, were presented with one 5-d-old *Canton S* male. Matings were observed and scored for 1 h (Fig. 2*B*) or 2 h (*SI Appendix*, Figs. S2C and S4*B*).

Statistical significance of our results was assessed using Fisher's exact test. * in Fig. 2*B* and *SI Appendix*, Fig. S2C means that the D1:Gal4/UAS-RNAi line result was significantly different from both control lines (D1:GAL4/+ and UAS-RNAi/+) from the same day. For CG9029, P value is ≤0.0001 for both RNAi lines versus all controls. All P values are shown in *SI Appendix*.

Sperm-Competition Assays. This assay and the statistical analysis of the results are described in detail in *SI Appendix*. In summary, single pair matings of *cn bw* females to tester males, secondary rematings to *cn bw* male (3 d later), fly handling, and progeny counting was performed as in ref. 35. Experiments presented in Fig. 4*B* were performed in two blocks. For the first block, we compared P1 between *ΔMSAmiP*-mutant and *exon8 wt-rescue*. For the second block we compared P1 between *ΔMSAmiP*, *exon8 wt-rescue*, and *MSAmiP-GFP* knockin. We performed two replicates for block 1, with sample sizes: MSAmiP-mutant n = 40 for replicate 1 and n = 22 for replicate 2; and WT rescue n = 38 for replicate 1 and n = 29 for replicate 2MSAmiP. For block 2, we performed two replicates, each with a smaller sample size (total sample size MSAmiP mutant n = 28; MSAmiP-GFP n = 35; WT rescue n = 25). We performed a statistical test in R using the packages lme4 and emmeans (73–75). We tested if the proportion of offspring sired by the first male differed depending on the genotype of the first male (*ΔMSAmiP*, *MSAmiP-GFP*, or *exon8wt-rescue*) using a generalized linear mixed model (GLMM), assuming a binomial distribution of the data, adding "female ID," "replicate," and "block" as random effects. A subsequent experiment presented in *SI Appendix*, Fig. S4C was carried out, following similar procedures although in different laboratories, on the MSAmiP*3-GFP mutant (*SI Appendix*, *Methods*).

Data Availability. The data discussed in this publication have been deposited in NCBI's Gene Expression Omnibus (76) and are accessible through GEO Series accession number GSE165066 (77).

GENETICS

ACKNOWLEDGMENTS. We are indebted to Daniel Pauli for stimulating discussions, and we thank Fabienne Cléard, Annick Mutero, Jorge Faustino, and Eva Favre for technical help. We thank the Cornell Statistical Consulting Unit for consultation, the Flow Cytometry core facility of the University of Geneva for secondary cell sorting, the iGE3 genomics platform for RNA sequencing, and Federico Miozzo for his help with RNAseq data analysis. C.I. thanks the members of François Payre laboratory and Muriel Boube for comments on the manuscript. This work was funded by the State of Geneva (to C.I., E.N., F.K., P.M.A., R.K.M., and Y.F.), the Swiss National Fund for Research (http://www.snf.ch) to F.K. and R.K.M. (31003A_149634), to R.K.M. (310030_192621), and to E.N. (31003A_169548), and finally, donations from the Claraz Foundation (to F.K.). Parts of this work were funded by the NIH (https://www.nih.gov/); (Grant R01-HD059060 to M.F.W. and Andrew G. Clark) and the NSF REU grant (PIs: J. Liu and V. Vogt) which supported J.G.

1. C. P. Ponting, P. L. Oliver, W. Reik, Evolution and functions of long noncoding RNAs. *Cell* **136**, 629–641 (2009).
2. J. I. Pueyo, E. G. Magny, J. P. Couso, New peptides under the s(ORF)ace of the genome. *Trends Biochem. Sci.* **41**, 665–678 (2016).
3. J. P. Kastenmayer *et al*., Functional genomics of genes with small open reading frames (sORFs) in S. cerevisiae. *Genome Res.* **16**, 365–373 (2006).
4. K. Hanada, X. Zhang, J. O. Borevitz, W. H. Li, S. H. Shiu, A large number of novel coding small open reading frames in the intergenic regions of the Arabidopsis thaliana genome are transcribed and/or under purifying selection. *Genome Res.* **17**, 632–640 (2007).
5. S. A. Slavoff *et al*., Peptidomic discovery of short open reading frame-encoded peptides in human cells. *Nat. Chem. Biol.* **9**, 59–64 (2013).
6. J. L. Aspden *et al*., Extensive translation of small open reading frames revealed by poly-ribo-seq. *eLife* **3**, e03528 (2014).
7. N. T. Ingolia *et al*., Ribosome profiling reveals pervasive translation outside of annotated protein-coding genes. *Cell Rep.* **8**, 1365–1379 (2014).
8. D. Lauressergues *et al*., Primary transcripts of microRNAs encode regulatory peptides. *Nature* **520**, 90–93 (2015).
9. S. Prabakaran *et al*., Quantitative profiling of peptides from RNAs classified as noncoding. *Nat. Commun.* **5**, 5429 (2014).
10. E. Ladoukakis, V. Pereira, E. G. Magny, A. Eyre-Walker, J. P. Couso, Hundreds of putatively functional small open reading frames in Drosophila. *Genome Biol.* **12**, R118 (2011).
11. A. de Andres-Pablo, A. Morillon, M. Wery, LncRNAs, lost in translation or licence to regulate? *Curr. Genet.* **63**, 29–33 (2017).
12. S. J. Andrews, J. A. Rothnagel, Emerging evidence for functional peptides encoded by short open reading frames. *Nat. Rev. Genet.* **15**, 193–204 (2014).
13. K. Hanyu-Nakamura, H. Sonobe-Nojima, A. Tanigawa, P. Lasko, A. Nakamura, Drosophila Pgc protein inhibits P-TEFb recruitment to chromatin in primordial germ cells. *Nature* **451**, 730–733 (2008).
14. T. Kondo *et al*., Small peptides switch the transcriptional activity of Shavenbaby during Drosophila embryogenesis. *Science* **329**, 336–339 (2010).
15. T. Kondo *et al*., Small peptide regulators of actin-based cell morphogenesis encoded by a polycistronic mRNA. *Nat. Cell Biol.* **9**, 660–665 (2007).
16. J. Zanet *et al*., Pri sORF peptides induce selective proteasome-mediated protein processing. *Science* **349**, 1356–1358 (2015).
17. J. I. Pueyo *et al*., Hemotin, a regulator of phagocytosis encoded by a small ORF and conserved across metazoans. *PLoS Biol.* **14**, e1002395 (2016).
18. E. G. Magny *et al*., Conserved regulation of cardiac calcium uptake by peptides encoded in small open reading frames. *Science* **341**, 1116–1120 (2013).
19. C. Wilson, A. Leiblich, D. C. Goberdhan, F. Hamdy, The Drosophila accessory gland as a model for prostate cancer and other pathologies. *Curr. Top. Dev. Biol.* **121**, 339–375 (2017).
20. B. A. Laflamme, M. F. Wolfner, Identification and function of proteolysis regulators in seminal fluid. *Mol. Reprod. Dev.* **80**, 80–101 (2013).
21. F. W. Avila, L. K. Sirot, B. A. LaFlamme, C. D. Rubinstein, M. F. Wolfner, Insect seminal fluid proteins: Identification and function. *Annu. Rev. Entomol.* **56**, 21–40 (2011).
22. I. Carmel, U. Tram, Y. Heifetz, Mating induces developmental changes in the insect female reproductive tract. *Curr. Opin. Insect Sci.* **13**, 106–113 (2016).
23. G. P. League, L. L. Baxter, M. F. Wolfner, L. C. Harrington, Male accessory gland molecules inhibit harmonic convergence in the mosquito Aedes aegypti. *Curr. Biol.* **29**, R196–R197 (2019).
24. E. C. Degner *et al*., Proteins, transcripts, and genetic architecture of seminal fluid and sperm in the mosquito *Aedes aegypti*. *Mol. Cell. Proteomics* **18** (suppl. 1), S6–S22 (2019).
25. N. Wedell, Female receptivity in butterflies and moths. *J. Exp. Biol.* **208**, 3433–3440 (2005).
26. A. Bairati, Structure and ultrastructure of the male reproductive system in Drosophila melanogaster. II. the genital duct and accessory glands. *Monit. Zool. Ital.* **2**, 105–182 (1968).
27. E. Prince *et al*., Rab-mediated trafficking in the secondary cells of Drosophila male accessory glands and its role in fecundity. *Traffic* **20**, 137–151 (2019).
28. L. Corrigan *et al*., BMP-regulated exosomes from Drosophila male reproductive glands reprogram female behavior. *J. Cell Biol.* **206**, 671–688 (2014).
29. M. J. Bertram, G. A. Akerkar, R. L. Ard, C. Gonzalez, M. F. Wolfner, Cell type-specific gene expression in the Drosophila melanogaster male accessory gland. *Mech. Dev.* **38**, 33–40 (1992).
30. M. Ottiger, M. Soller, R. F. Stocker, E. Kubli, Binding sites of Drosophila melanogaster sex peptide pheromones. *J. Neurobiol.* **44**, 57–71 (2000).
31. E. Kubli, D. Bopp, Sexual behavior: How sex peptide flips the postmating switch of female flies. *Curr. Biol.* **22**, R520–R522 (2012).
32. H. Liu, E. Kubli, Sex-peptide is the molecular basis of the sperm effect in Drosophila melanogaster. *Proc. Natl. Acad. Sci. U.S.A.* **100**, 9929–9933 (2003).
33. J. Peng *et al*., Gradual release of sperm bound sex-peptide controls female postmating behavior in Drosophila. *Curr. Biol.* **15**, 207–213 (2005).
34. J. L. Sitnik, D. Gligorov, R. K. Maeda, F. Karch, M. F. Wolfner, The female post-mating response requires genes expressed in the secondary cells of the male accessory gland in Drosophila melanogaster. *Genetics* **202**, 1029–1041 (2016).
35. D. Gligorov, J. L. Sitnik, R. K. Maeda, M. F. Wolfner, F. Karch, A novel function for the Hox gene Abd-B in the male accessory gland regulates the long-term female postmating response in Drosophila. *PLoS Genet.* **9**, e1003395 (2013).
36. A. Singh *et al*., Long-term interaction between Drosophila sperm and sex peptide is mediated by other seminal proteins that bind only transiently to sperm. *Insect Biochem. Mol. Biol.* **102**, 43–51 (2018).
37. K. R. Ram, M. F. Wolfner, Sustained post-mating response in Drosophila melanogaster requires multiple seminal fluid proteins. *PLoS Genet.* **3**, e238 (2007).
38. R. K. Maeda *et al*., The lncRNA male-specific abdominal plays a critical role in Drosophila accessory gland development and male fertility. *PLoS Genet.* **14**, e1007519 (2018).
39. R. Minami *et al*., The homeodomain protein defective proventriculus is essential for male accessory gland development to enhance fecundity in Drosophila. *PLoS One* **7**, e32302 (2012).
40. C. Immarigeon, F. Karch, R. K. Maeda, FACS-based isolation and RNA extraction of secondary cells from the Drosophila male accessory gland. *bioRxiv* [Preprint] (2019).
41. A. Thomas *et al*., A versatile method for cell-specific profiling of translated mRNAs in Drosophila. *PLoS One* **7**, e40276 (2012).
42. B. Bertin, Y. Renaud, R. Aradhya, K. Jagla, G. Junion, TRAP-rc, translating ribosome affinity purification from rare cell populations of Drosophila embryos. *J. Vis. Exp.* 52985 (2015).
43. G. D. Findlay, X. Yi, M. J. Maccoss, W. J. Swanson, Proteomics reveals novel Drosophila seminal fluid proteins transferred at mating. *PLoS Biol.* **6**, e178 (2008).
44. G. D. Findlay, M. J. MacCoss, W. J. Swanson, Proteomic discovery of previously unannotated, rapidly evolving seminal fluid genes in Drosophila. *Genome Res.* **19**, 886–896 (2009).
45. G. D. Findlay *et al*., Evolutionary rate covariation identifies new members of a protein network required for Drosophila melanogaster female post-mating responses. *PLoS Genet.* **10**, e1004108 (2014).
46. T. Chapman *et al*., The sex peptide of Drosophila melanogaster: Female post-mating responses analyzed by using RNA interference. *Proc. Natl. Acad. Sci. U.S.A.* **100**, 9923–9928 (2003).
47. S. Redhai *et al*., Regulation of dense-core granule replenishment by autocrine BMP signalling in Drosophila secondary cells. *PLoS Genet.* **12**, e1006366 (2016).
48. B. R. Hopkins *et al*., BMP signaling inhibition in *Drosophila* secondary cells remodels the seminal proteome and self and rival ejaculate functions. *Proc. Natl. Acad. Sci. U.S.A.* **116**, 24719–24728 (2019).
49. M. Gummalla *et al*., abd-A regulation by the iab-8 noncoding RNA. *PLoS Genet.* **8**, e1002720 (2012).
50. S. Kondo *et al*., New genes often acquire male-specific functions but rarely become essential in *Drosophila*. *Genes Dev.* **31**, 1841–1846 (2017).
51. J. Bischof, R. K. Maeda, M. Hediger, F. Karch, K. Basler, An optimized transgenesis system for Drosophila using germ-line-specific phiC31 integrases. *Proc. Natl. Acad. Sci. U.S.A.* **104**, 3312–3317 (2007).
52. E. Boorman, G. A. Parker, Sperm (ejaculate) competition in Drosophila melanogaster, and the reproductive value of females to males in relation to female age and mating status. *Ecol. Entomol.* **1**, 145–155 (1976).
53. L. G. Harshman, T. Prout, Sperm displacement without sperm transfer in Drosophila melanogaster. *Evolution* **48**, 758–766 (1994).
54. A. G. Clark, M. Aguadé, T. Prout, L. G. Harshman, C. H. Langley, Variation in sperm displacement and its association with accessory gland protein loci in Drosophila melanogaster. *Genetics* **139**, 189–201 (1995).
55. K. A. Hughes, Quantitative genetics of sperm precedence in Drosophila melanogaster. *Genetics* **145**, 139–151 (1997).
56. F. W. Avila, K. Ravi Ram, M. C. Bloch Qazi, M. F. Wolfner, Sex peptide is required for the efficient release of stored sperm in mated Drosophila females. *Genetics* **186**, 595–600 (2010).
57. M. F. Wolfner, Tokens of love: Functions and regulation of Drosophila male accessory gland products. *Insect Biochem. Mol. Biol.* **27**, 179–192 (1997).
58. S. Wigby, T. Chapman, Sperm competition. *Curr. Biol.* **14**, R100–R102 (2004).
59. M. K. Manier *et al*., Resolving mechanisms of competitive fertilization success in Drosophila melanogaster. *Science* **328**, 354–357 (2010).
60. N. M. Seibel, J. Eljouni, M. M. Nalaskowski, W. Hampe, Nuclear localization of enhanced green fluorescent protein homomultimers. *Anal. Biochem.* **368**, 95–99 (2007).
61. F. W. Avila, A. L. Mattei, M. F. Wolfner, Sex peptide receptor is required for the release of stored sperm by mated Drosophila melanogaster females. *J. Insect Physiol.* **76**, 1–6 (2015).
62. J. L. Mueller, J. R. Linklater, K. Ravi Ram, T. Chapman, M. F. Wolfner, Targeted gene deletion and phenotypic analysis of the Drosophila melanogaster seminal fluid protease inhibitor Acp62F. *Genetics* **178**, 1605–1614 (2008).

63. O. Lung, M. F. Wolfner, Drosophila seminal fluid proteins enter the circulatory system of the mated female fly by crossing the posterior vaginal wall. *Insect Biochem. Mol. Biol.* **29**, 1043–1052 (1999).
64. S. Misra, M. F. Wolfner, *Drosophila* seminal sex peptide associates with rival as well as own sperm, providing SP function in polyandrous females. *eLife* **9**, 1–21 (2020).
65. J. Wang *et al*., ncRNA-encoded peptides or proteins and cancer. *Mol. Ther.* **27**, 1718–1725 (2019).
66. J. Z. Huang *et al*., A peptide encoded by a putative lncRNA HOXB-AS3 suppresses colon cancer growth. *Mol. Cell* **68**, 171–184.e6 (2017).
67. M. McVey, D. Radut, J. J. Sekelsky, End-joining repair of double-strand breaks in Drosophila melanogaster is largely DNA ligase IV independent. *Genetics* **168**, 2067–2076 (2004).
68. D. M. Tyler *et al*., Functionally distinct regulatory RNAs generated by bidirectional transcription and processing of microRNA loci. *Genes Dev.* **22**, 26–36 (2008).
69. A. Stark *et al*., A single Hox locus in Drosophila produces functional microRNAs from opposite DNA strands. *Genes Dev.* **22**, 8–13 (2008).
70. M. Ronshaugen, F. Biemar, J. Piel, M. Levine, E. C. Lai, The Drosophila microRNA iab-4 causes a dominant homeotic transformation of halteres to wings. *Genes Dev.* **19**, 2947–2952 (2005).
71. W. Bender, MicroRNAs in the Drosophila bithorax complex. *Genes Dev.* **22**, 14–19 (2008).
72. D. L. Garaulet *et al*., Homeotic function of Drosophila Bithorax-complex miRNAs mediates fertility by restricting multiple Hox genes and TALE cofactors in the CNS. *Dev. Cell* **29**, 635–648 (2014).
73. D. Bates, M. Mächler, B. Bolker, S. Walker, Fitting linear mixed-effects models using lme4. *J. Stat. Software* **67**, 48 (2015).
74. R Core Team, R: A Language and Environment for Statistical Computing (R Foundation Statistical Computing, Vienna, Austria, 2020). https://www.R-project.org/. Accessed 29 March 2021.
75. R. V. Length. Emmeans: Estimated Marginal Means, aka Least-Squares Means (Version 1.1.1, R package, 2019, CRAN).
76. R. Edgar, M. Domrachev, A. E. Lash, Gene Expression Omnibus: NCBI gene expression and hybridization array data repository. *Nucleic Acids Res.* **30**, 207–210 (2002).
77. C. Immarigeon, R. K. Maeda, F. Karch, RNA-seq and Ribosome immunoprecipitation results from purified Drosophila male secondary cells. *Gene Expression Omnibus*. https://www.ncbi.nlm.nih.gov/geo/query/acc.cgi?acc=GSE165066. Deposited 20 January 2021.
78. A. H. Brand, N. Perrimon, Targeted gene expression as a means of altering cell fates and generating dominant phenotypes. *Development* **118**, 401–415 (1993).